Influence of gp41 Fusion Peptide on the Kinetics of Poly(ethylene glycol)-Mediated Model Membrane Fusion†

Md. Emdadul Haque and Barry R. Lentz*

Department of Biochemistry and Program in Molecular/Cell Biophysics, University of North Carolina, Chapel Hill, North Carolina 27599-7260

Received April 8, 2002; Revised Manuscript Received July 3, 2002

ABSTRACT: The fusion peptide of the HIV fusion protein gp41 is required for viral fusion and entry into a host cell, but it is unclear whether this 23-residue peptide can fuse model membranes. We address this question for model membrane vesicles in the presence and absence of aggregating concentrations of poly(ethylene glycol) (PEG). PEG had no effect on the physical properties of peptide bound to membranes or free in solution. We tested for fusion of both highly curved and uncurved PC/PE/SM/CH (35:30:15:20 mol %) vesicles and highly curved PC/PE/CH (1:1:1) vesicles treated with peptide in the presence and absence of PEG. Fusion was never observed in the absence of PEG, although high peptide concentrations led to aggregation and rupture, especially in unstable PC/PE/CH (1:1:1) vesicles. When 5 wt % PEG was present to aggregate vesicles, peptide enhanced the rate of lipid mixing between curved PC/PE/SM/CH vesicles in proportion to the peptide concentration, with this effect leveling off at peptide/lipid (P/L) ratios ≈1:200. Peptide produced an even larger effect on the rate of contents mixing but inhibited contents mixing at P/L ratios >1:200. No fusion enhancement was seen with uncurved vesicles. The rate of fusion was also enhanced by the presence of hexadecane, and peptide-induced rate enhancement was not observed in the presence of hexadecane. We conclude that gp41 fusion peptide does not induce vesicle fusion at subrupturing concentrations but can enhance fusion between highly curved vesicles induced to fuse by PEG. The different effects of peptide on the rates of lipid mixing and fusion pore formation suggest that, while gp41 fusion peptide does affect hemifusion, it mainly affects pore formation.

Virus−cell membrane fusion is an essential and important step for the infectious entry of a virus into a host cell. Viral fusion proteins are the machines that drive the fusion process during viral entry. The envelope glycoprotein of HIV[1] is a fusion machine that is expressed as a polypeptide precursor, gp160, which is cleaved to two noncovalently associated subunits, gp120 and gp41 (*28*, *57*). Upon binding of gp120 to the cell surface receptor, CD4, gp41 undergoes conformational changes to become active in promoting virus−cell membrane fusion (*17*, *35*, *75*). The N-terminus of gp41 contains an amphipathic, glycine-rich, 20−25 amino acid residue peptide ("fusion peptide") that is required for fusion activity (*57*).

The amino acid sequence and crystallographic structure of the ectodomain of many viral proteins including gp41 of HIV (*8*, *73*) are known. Despite this structural information and what is a reasonable picture of how protein fusion machines bring membranes into contact and perturb them (*42*), we have no real information on the role of the fusion peptides in protein-mediated fusion. Several viral fusion proteins containing a fusion peptide are known to promote the fusion process; those of influenza virus (*9*, *19*, *39*, *49*, *56*, *68*, *74*), simian immunodeficiency virus (*5*, *51*), and human immunodeficiency virus (HIV) (*18*, *22*, *45*) are well documented. Despite clear evidence of the importance of the N-terminal fusion peptide to viral fusion, there is uncertainty as to whether this 23 amino acid residue peptide, on its own, induces fusion of pure lipid bilayers.

gp41 fusion peptide interacts with the outer leaflet of liposome membranes (*6*) to induce aggregation, leakage of trapped contents, and lipid mixing between model membranes (*31*, *50*, *59*−*61*, *63*, *67*, *70*). Lipid mixing and aggregation have almost universally been interpreted in terms of fusion, although none of these studies have reported gp41 fusion peptide-induced mixing of vesicle contents. Of course, the universally accepted and the only incontrovertible demonstration of fusion is contents mixing in the absence of extensive loss of trapped contents. Thus, *we ask whether*

† Supported by USPHS Grant GM 32707 to B.R.L.

* To whom correspondence and requests for reprints should be addressed. E-mail: uncbrl@med.unc.edu. Telephone: 919-966-5384. Fax: 919-966-2852.

[1] Abbreviations: SUVs, small unilamellar vesicles; LUVs, large unilamellar vesicles; HIV, human immunodeficiency virus; HA, hemagglutinin; gp41, 41000 Da subunit of the HIV fusion protein; QELS, quasi-elastic light scattering; DOPC, 1,2-dioleoyl-3-*sn*-phosphatidylcholine; DOPE, 1,2-dioleoyl-3-*sn*-phosphatidylethanolamine; POPG, palmitoyloleoylphosphatidylglycerol; POPC, palmitoyloleoylphosphatidylcholine; SM, sphingomyelin (bovine brain); CH, cholesterol; 6,7-Br_2-PC, 1-palmitoyl-2-stearoyl-6,7-dibromo-3-*sn*-phosphatidylcholine; 11,12-Br_2-PC, 1-palmitoyl-2-stearoyl-11,12-dibromo-3-*sn*-phosphatidylcholine; BODIPY530/550 C_{12}-HPE, 2-(4,4-difluoro-5,7-diphenyl-4-bora-3a,4a-diaza-*s*-indacene-3-dodecanoyl)-1-hexadecanoyl-*sn*-glycero-3-phosphoethanolamine; *β*-BODIPY500/510 C_{12}-HPC, 2-(4,4-difluoro-5,7-diphenyl-4-bora-3a,4a-diaza-*s*-indacene-3-dodecanoyl)-1-hexadecanoyl-*sn*-glycero-3-phosphocholine; $C_{12}E_8$, dodecyloctaethylene glycol monoether; Tb^{3+}, terbium; DPA, pyridine-2,6-dicarboxylic acid; TES, *N*-[tris(hydroxymethyl)methyl]-2-aminoethanesulfonic acid; PEG, poly(ethylene glycol); CM, contents mixing; LM, lipid mixing.

10.1021/bi020269q CCC: $22.00 © 2002 American Chemical Society
Published on Web 08/07/2002

gp41 fusion peptide actually induces membrane fusion or aggregation and rupture of model membrane vesicles.

It is generally accepted that membrane-disruptive peptide/lipid (P/L) ratios (>1:50) are needed to elicit gp41-mediated vesicle aggregation (*60*), and since aggregation is a prerequisite to fusion, these ratios are usually seen as needed to induce "fusion" (usually defined as lipid mixing and contents leakage). Only one study showed that the gp41 fusion peptide (at moderate P/L ratios <1:100) actually induced contents mixing without extensive leakage (the accepted definition of fusion) between palmitoyloleoylphosphatidylglycerol (POPG)[1] vesicles, but only in the presence of Ca^{2+}, presumably to trigger a conformational change in the fusion peptide (*58*). However, Ca^{2+} also aggregated but did not fuse the negatively charged POPG vesicles (*58*). While Ca^{2+}-induced conformational changes may have been important in explaining these results, we suspect that it was Ca^{2+}-induced vesicle aggregation that made possible fusion peptide-induced fusion of POPG. To test this, *we ask whether even low peptide concentrations might induce or enhance fusion of vesicles already aggregated by poly(ethylene glycol) (PEG)[1]?*

It is well know that fusion is promoted by membrane curvature stress, such as occurs in sonicated small unilamellar vesicles (SUVs)[1] (*41*, *43*). However, most studies of the influence of HIV peptide on membranes have been performed with relatively uncurved large unilamellar vesicles (LUVs)[1] (*1*, *31*, *50*, *52*, *58*−*63*, *70*), although many papers have used LUVs and SUVs interchangeably (*31*, *50*, *62*, *63*). In a recent study of influenza virus hemagglutinin (HA)[1] fusion peptide, we showed that the ability of this fusion peptide to enhance fusion of PEG-aggregated vesicles required SUVs (*23*). *We ask here whether the same requirement for a mechanically stressed and curved membrane exists for the fusion-enhancing activity of the gp41 fusion peptide*.

Membrane lipid composition is also reported to affect the interaction of gp41 fusion peptide with vesicles. Acidic lipids were initially reported as required for the interaction of HIV-1 gp41 fusion peptide with vesicles (*63*), but later work showed unequivocally that neutral lipid vesicles were also aggregated, disrupted, and induced to mix their lipids (*1*, *16*, *50*, *60*, *61*). Because phosphatidylethanolamine was reported as necessary for gp41 fusion peptide insertion into a bilayer (*50*), many recent studies have used vesicle composed of a 1:1:1 mixture of dioleoylphosphatidylcholine (DOPC)[1]/dioleoylphosphatidylethanolamine (DOPE)[1]/cholesterol (CH)[1]. Vesicles prepared from this mixture were easily aggregated and disrupted by gp41 fusion peptide, leading to the current view that the role of fusion peptide is to disrupt membranes containing mixtures of these three lipids (*50*, *52*, *60*, *61*). However, we have recently shown that this particular mix of lipids, whether incorporated into SUVs or LUVs, is unstable and that a somewhat different mix of DOPC/DOPE/sphingomyelin (SM)[1]/CH (35:30:15:20 mol ratio) is optimally fusogenic in the sense that it maximized fusion while minimizing leakage of contents and mimics the composition of synaptic vesicles and other cell membranes (*24*). *Here we ask whether vesicles with these two lipid compositions are affected similarly by gp41 fusion peptide*.

While most studies of the effects of gp41 peptide have concluded that it acts to promote fusion by destabilizing the bilayer (*50*, *60*), results obtained with cells expressing mutant HA fusion machines have concluded that the fusion peptide promotes formation of a mature fusion pore (*64*). *We also ask whether gp41 fusion peptide acts by destabilizing the bilayer (i.e., by promoting lipid mixing) or by promoting a later step in the fusion process*.

EXPERIMENTAL PROCEDURES

Materials

Chloroform stock solutions of 1,2-dioleoyl-3-*sn*-phosphatidylcholine (DOPC),[1] 1,2-dioleoyl-3-*sn*-phosphatidylethanolamine (DOPE),[1] sphingomyelin (bovine brain, SM),[1] 1-palmitoyl-2-stearoyl-6,7-dibromo-3-*sn*-phosphatidylcholine (6,7-Br_2-PC),[1] 1-palmitoyl-2-stearoyl-11,12-dibromo-3-*sn*-phosphatidylcholine (11,12-Br_2-PC)[1] were purchased from Avanti Polar Lipids, Inc. (Birmingham, AL) and used without further purification. The concentrations of all of the stock lipids were determined by phosphate assay (*11*). Cholesterol (CH)[1] was purchased from Avanti Polar Lipids and was further purified as previously reported by Schwenk et al. (*65*). 1,6-Diphenyl-1,3,5-hexatriene (DPH), 2-(4,4-difluoro-5,7-diphenyl-4-bora-3a,4a-diaza-*s*-indacene-3-dodecanoyl)-1-hexadecanoyl-*sn*-glycero-3-phosphoethanolamine (*β*-BODIPY530/550 C_{12}-HPE),[1] and 2-(4,4-difluoro-5,7-diphenyl-4-bora-3a,4a-diaza-*s*-indacene-3-dodecanoyl)-1-hexadecanoyl-*sn*-glycero-3-phosphocholine (*β*-BODIPY500/510 C_{12}-HPC)[1] were purchased from Molecular Probes (Eugene, OR). Terbium (Tb^{3+}) chloride was purchased from Johnson Matthey Co. (Ward Hill, MA). Dipicolinic acid (DPA)[1] and *N*-[tris(hydroxymethyl)methyl]-2-aminoethanesulfonic acid (TES)[1] were purchased from Sigma Chemical Co. (St. Louis, MO). Poly(ethylene glycol) of molecular weight 7000−9000 (PEG[1] 8000) was purchased from Fisher Scientific (Fairlane, NJ) and further purified as previously reported (*43*). Dodecyloctaethylene glycol monoether ($C_{12}E_8$)[1] was purchased from Calbiochem (La Jolla, CA). All other reagents were of the highest purity grade available.

Methods

Preparation of gp41 Fusion Peptide. The N-terminus of the HIV gp41 fusion peptides (native and mutant) were chemically synthesized and purified by the peptide synthesis laboratory of UNC-CH. The sequences of the peptides are AVGIGAL**F**LGFLGAAGSTMGARS (native) and AVGIGAL**W**LGFLGAAGSTMGARS (mutant F8W). The peptides were synthesized by the standard solid-phase method on a Biosearch model 9500 peptide synthesizer (PerSeptive Biosystems) using *t*-Boc chemistry. The peptide was purified by HPLC (Rainin, Emeryville, CA) on a C18 Vydac column. Amino acid determination and mass spectroscopy confirmed the peptide identity and showed the dried product to be >90 wt % of the desired peptide. For all experiments, the stock peptide solutions were prepared in DMSO solvent. DMSO constituted up to 1.25% of the buffer volume at the completion of the binding titrations, while all other experiments were done using less than 1% of the total volume of vesicle suspension. We performed control experiments for leakage, contents mixing, and lipid mixing in the presence of 1% DMSO and showed that this amount of DMSO had no effect on fusion and leakage. All experiments were done using the wild-type peptide except for the binding and depth

of penetration experiments, for which the Trp residue was required for detection. Recently, Agirre et al. (*1*) reported that this Trp mutant of gp41 fusion peptide behaves similarly to the wild-type peptide (similar lipid mixing and binding). In addition, while others report that mutations in valine-2 and phenylalanine-11 of gp41 fusion affect the efficiency of leakage and lipid mixing, they did not alter the membrane binding or conformation of the gp41 peptide (*31*, *60*, *62*).

Peptide Binding. Membrane binding in the presence and absence of PEG (10 w/w %) was detected by energy transfer from the peptide tryptophan to membrane-associated DPH (250:1 lipid/probe) as peptide was added to SUVs. Control experiments were identical except that SUVs were prepared without DPH. Tryptophan was excited at 280 nm and emission spectra were recorded from 295 to 540 nm using a monochromator and instrument slit widths of 4/4 for both the excitation and emission light. The control spectrum (no probe) was subtracted from the spectrum in the presence of probe to obtain the fluorescence intensity change at λ_{max} of DPH. Data sets obtained at two membrane concentrations (500 and 250 μM) were fitted globally using Sigma Plot 2000 to determine binding parameters (*32*).

Penetration of Mutant Peptide Tryptophan into Membranes. We have measured the depth of penetration of the single tryptophan residue in F8W gp41 fusion peptide into vesicle bilayers using the parallax method (*10*). Lipids brominated at the 6,7 and 11,12 positions in the acyl chain were used as tryptophan quenchers. For this measurement, we used 20 mol % Br-PC as a substitute for part of the DOPC in our optimally fusogenic lipid mix. Aliquots of the peptide solution were added to vesicles to achieve a final P/L ratio of 1:400 and incubated for 10 min before tryptophan fluorescence intensity was recorded. Fluorescence was measured at 23 °C with a SLM 48000 spectrofluorometer (SLM Aminco, Urbana, IL) operating in the T-format and using 1 cm path-length quartz cuvettes. An excitation wavelength of 280 nm was used, with excitation and emission slits set at 4/4 nm. Control readings were obtained in the absence of peptide and subtracted from sample readings. The location of tryptophan relative to the center of the bilayer was calculated as (*10*)

$$Z_{cF} = L_{c1} + \{[(-1/\pi C)\ln(F_1/F_2) - L_{21}^2]/2L_{21}\}$$

where L_{c1} = the distance of the center of the bilayer from the shallow quencher 1, L_{21} = the difference in depth between the two quenchers, and C = the two-dimensional quencher concentration in the plane of the membrane. F_1 and F_2 are normalized fluorescence intensities of samples having quenchers located at different depths in the bilayer. The average bromine distances from the center of the bilayer were taken from the literature (10.8 and 6.3 Å for the 6,7-BrPC and 11,12-BrPC, respectively) (*55*). The cross-sectional area of one lipid molecule was taken as 70 Å^2 (*27*).

Vesicle Preparation. Mixtures of different lipids at appropriate molar ratios in chloroform were dried under nitrogen. The dried mixed lipids were dissolved in 1 mL of cyclohexane containing a small aliquot of methanol, frozen in a shell on the surface of a small vial using dry ice, and dried under high vacuum overnight. The freeze-dried lipids were easily suspended in an appropriate aqueous buffer above the main lipid phase transition. For SUV preparation, the lipid suspension was maintained at 4 °C and sonicated for 15 min at a 50% duty cycle for using a Heat Systems model 350 sonicator (Plainview, NY) equipped with a titanium probe tip. Vesicles were fractionated by centrifugation at 70000 rpm for 25 min at 4 °C using a Beckman TL-100 ultracentrifuge (Palo Alto, CA). Large unilamellar vesicles were prepared by extruding (*26*, *54*) lipid suspensions 10 times through a 0.1 μm polycarbonate filter (Nucleo Pore Corp., Pleasanton, CA) at room temperature under a pressure of 100 psi of nitrogen.

Contents Mixing and Leakage Assays. The Tb/DPA contents mixing and leakage assays were based on those originally proposed by Wilschut et al. (*76*) and adapted to monitor PEG-induced fusion (*71*). Vesicles were prepared in either 80 mM DPA or 8 mM $TbCl_3$ plus 60 mM sodium citrate and 10 mM TES, pH 7.4, and untrapped, probe-containing buffer was removed from the vesicles using a Sephadex G-75 column equilibrated with assay buffer (100 mM NaCl, 10 mM TES, 1 mM EDTA, and 1 mM $CaCl_2$). The lipid concentration in all experiments was 0.2 mM.

To measure the mixing of vesicle contents due to fusion, stock PEG solutions were added with rapid stirring to a mixture (1:1) of the Tb- and DPA-containing vesicles, and the kinetics of vesicles fusion were measured in terms of an increase in Tb^{3+} fluorescence intensity due to formation of the Tb/DPA complex with time. For experiments with peptide, this was added to the Tb- and DPA-containing vesicle solutions just prior to the addition of PEG solution. $C_{12}E_8$ detergent was added to release the contents of the vesicles, and fluorescence intensity was once again recorded. The fluorescence of coencapsulated Tb/DPA vesicles was taken as indicative of 100% contents mixing, such that

$$\%\ \text{contents mixing (CM)} = \Delta F(\text{Tb} + \text{DPA};\ x\ \text{wt}\ \%\ \text{PEG})/\Delta F(\text{Tb/DPA};\ x\ \text{wt}\ \%\ \text{PEG})$$

Details of this procedure are described by Talbot et al. (*71*).

Leakage of contents was followed using vesicles containing coencapsulated 4 mM $TbCl_3$, 40 mM (DPA),[1] 30 mM sodium citrate, and 10 mM TES, pH 7.4. When leakage of contents occurred, there was a drop in fluorescence due to Tb^{3+} quenching by water (*69*) when the trapped compartment was diluted into the external compartment. The fluorescence intensity of the coencapsulated Tb/DPA vesicles suspended in a subfusion PEG concentration was taken as indicating 0% leakage. The fluorescence intensity of Tb/DPA vesicles after treatment with 0.45 mM $C_{12}E_8$ (20 μL of 80 mM $C_{12}E_8$ added to 2 mL of vesicle suspension) was taken to indicate 100% leakage of trapped contents.

Lipid Mixing Assay. Fluorescent lipid probes with fluorophores attached to their acyl chains, BODIPY500-PC and BODIPY530-PE (Molecular Probes, Eugene, OR), were used for measuring lipid transfer during PEG- and peptide-mediated vesicle fusion (*47*). To measure lipid transfer during PEG/peptide-induced fusion, probe-containing vesicles were mixed with probe-free vesicles at a ratio of 1:4. PEG and/or peptide stock solutions were added to the vesicle mixtures, and the change of fluorescence intensity due to probe dilution was monitored with time. The emission intensities of donor and acceptor were recorded in T-format with channel A at 520 nm (slits 8 nm) and with a 550 nm cutoff filter (Schott

Glass Technologies, Duryea, PA) in channel B. Excitation was at 500 nm using slits of 4 nm. The ratio of donor/acceptor intensity was recorded, and the extent of lipid mixing was calculated using standard curves from such measurements with vesicles with known probe concentrations (*47*). It was assumed that 100% lipid mixing corresponded to a 5-fold dilution of the probe.

Vesicle Size Measurements. The diameters of vesicles were measured by quasi-elastic light scattering (QELS) using a Nicomp autocorrelator (Particle Sizing Systems Inc., Santa Barbara, CA) incorporated into a multiangle instrument constructed by us (*43*). Autocorrelation decays were analyzed with software supplied from Particle Sizing Systems using volume-weighted averages and solid particle mode, as appropriate for SUVs.

RESULTS

Binding of the F8W gp41 Fusion Peptide to PC/PE/SM/CH (35:30:15:20 mol %) SUV. Figure 1 shows the increase in fluorescence intensity of membrane-bound DPH as a result of energy transfer from bound peptides with increasing peptide concentration. Binding parameters were obtained from fitting the two data sets globally to a standard surface-binding model, a procedure that allows good estimates of binding parameters (*32*). The apparent K_d and stoichiometry (*N*, outer leaflet lipids/bound peptide) providing a best fit to the data were 3.3 ± 1.2 μM and 7.3 ± 0.3, respectively. These values were then used in published equations to estimate the fraction of SUV surface occupied (*32*). The aggregation of gp41 peptide in solution has been noted at very high peptide concentrations (1.25 mM), even in the presence of membranes (*16*). Our titration results saturated at twice the fluorescence at 500 μM lipid than at 250 μM lipid indicate that essentially all peptide was membrane bound under our conditions. Even in the absence of membranes, QELS results revealed no peptide aggregation up to peptide concentrations of 150 μM, well above the concentrations used in our studies.

Effects of gp41 Fusion Peptide on Vesicles in the Absence of PEG. Time courses of contents leakage, contents mixing, and lipid mixing in DOPC/DOPE/CH (1:1:1) SUV at 37 °C are plotted in Figure 2 at different peptide concentrations in the absence of PEG. We have chosen this vesicle composition in order to compare our results to the many studies of gp41 peptide published using this or similar compositions (*31*, *50*, *52*, *59*−*62*, *70*). Experiments were carried out at 37 °C for the same reason. Before describing the effects of gp41 fusion peptide on these vesicles, we note that this particular lipid composition produces unusually large sonicated vesicles (36 nm) that are unstable and spontaneously aggregate and transform to larger structures (*24*). Thus, spontaneous contents leakage and lipid mixing between these vesicles were seen in the absence of any peptide (Figure 2). The rates of spontaneous leakage and lipid mixing at 37 °C were 3 and 5 times higher than at 23 °C (insets to frames A and C of Figure 2; Table 1). These results show that DOPC/DOPE/CH SUVs transform spontaneously to larger structures but without maintenance of trapped contents (insignificant contents mixing) when kept for any significant time at 37 °C and transform slowly to these structures even at 23 °C.

The initial rates of leakage and lipid mixing at these two temperatures in the presence of gp41 peptide were obtained from the data in Figure 2 and are summarized in Table 1 at one P/L ratio, and the rates obtained at 37 °C are plotted versus P/L ratio in the right insets to Figure 2A,C. These

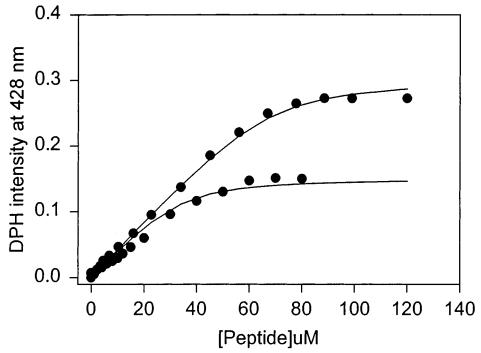

FIGURE 1: Peptide binding to PC/PE/SM/CH SUV. Peptide binding was detected by energy transfer from Trp to DPH as a function of peptide concentration at 23 °C. Measurements were carried out using 500 and 250 μM SUV (P/L ratio varied during the titration from 0−1 to 3−4 at saturation) in 10 mM TES, 100 mM NaCl, 1 mM Ca^{2+}, and 1 mM EDTA at pH 7.4. The smooth curves drawn through the data represent the best global fit of both data sets to a simple membrane binding model (*32*), yielding K_d = 3.3 ± 1.2 μM and stoichiometry (*N*) = 7.3 ± 0.3 outer leaflet lipids per peptide.

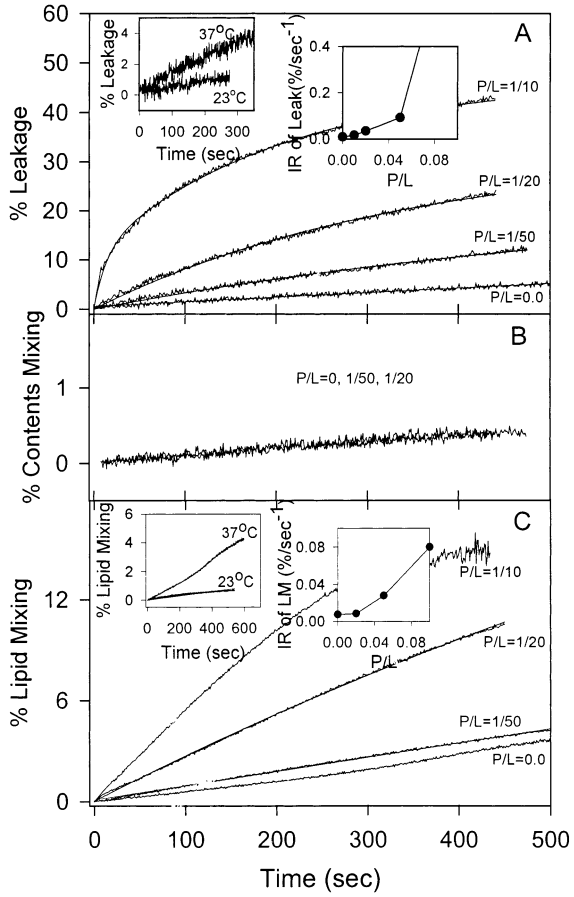

FIGURE 2: Time courses of (A) leakage, (B) contents mixing, and (C) lipid mixing for PC/PE/CH (1:1:1) SUV induced by the gp41 fusion peptide at 37 °C. Measurements ware carried out using 200 μM SUVs in 10 mM TES, 100 mM NaCl, 1 mM $CaCl_2$, and 1 mM EDTA, pH 7.4. Representative results are shown for different P/L ratios. The left insets compare the time courses of leakage and lipid mixing at 23 and 37 °C in the absence of peptide. The right insets show the initial rates of leakage and lipid mixing versus P/L ratio.

Table 1: Initial Rate of Leakage and Lipid Mixing of PC/PE/CH (1:1:1) and PC/PE/SM/CH SUV at Different Temperatures

	initial rate of leakage (s^{-1})		initial rate of lipid mixing (s^{-1})	
temp (°C)	with peptide[a]	no peptide	with peptide[a]	no peptide
PC/PE/CH				
37	0.05	9.3×10^{-3}	0.028	7.5×10^{-3}
23	0.01	3.8×10^{-3}	0.002	1.5×10^{-3}
PC/PE/SM/CH				
37	4.81×10^{-3}	2.81×10^{-3}	2.2×10^{-3}	1.04×10^{-3}
23	2.51×10^{-3}	1.1×10^{-3}	7.02×10^{-4}	0.56×10^{-3}

[a] P/L = 0.05.

data show that both peptide and increasing temperature stimulated spontaneous lipid rearrangements that led to vesicle aggregation and disruption and that the effect of peptide was enhanced at the higher temperature. The initial rate of leakage and lipid mixing increased slowly at low P/L ratio but increased dramatically at high P/L ratio (>0.04), indicating that high peptide concentration ruptures vesicles. However, it is also clear that the gp41 peptide had no effect on what was a very minimal rate of spontaneous contents mixing between these vesicles (Figure 2, frame B). Leakage (frame A) and lipid mixing (frame C), however, increased markedly with peptide concentration. Since contents mixing with minimal leakage is necessary and sufficient to demonstrate fusion, we must conclude that the gp41 fusion peptide was unable to induce fusion but was able to aggregate vesicles, induce lipid mixing, and destabilize DOPC/DOPE/CH SUV to produce larger structures (diameter changed from 48 to 168 nm at a L/P ratio of 20:1) in a dose-dependent manner. It has been suggested that peptide-mediated contents mixing cannot be detected because of the observed high peptide-induced leakage (*50*). However, contents leakage was sufficiently low at P/L ≤ 1:50 that we were able to correct our contents mixing assay (*43*), and we still observed no peptide-induced contents mixing. At higher P/L ratios (≥1:10), leakage increased substantially, and we could draw no clear conclusion about contents mixing.

Because DOPC/DOPE/CH vesicles are so unstable, we turned our attention to vesicles composed of a mixture of lipids that mimicked the composition of mammalian synaptic vesicles and that showed an optimal balance between contents mixing and leakage and were thus optimal for fusion (*24*). Figure 3 presents time courses of contents leakage (frame A), contents mixing (frame B), and lipid mixing (frame C) for DOPC/DOPE/SM/CH (35:30:15:20) SUVs at different peptide concentrations in the absence of PEG at 37 °C. It is immediately obvious that, in comparison to the DOPC/DOPE/CH SUVs described in Figure 2, these SUVs are much more stable (essentially zero contents mixing and very low leakage in the absence of peptide), although a small amount of spontaneous lipid mixing did occur, probably via the aqueous medium (*29*). As for DOPC/DOPE/CH vesicles, no mixing of contents was detected at any peptide concentration (up to P/L = 1:20). The rates of leakage and lipid mixing increased with increasing peptide concentrations (see insets to frames A and C). Experiments were also performed at 23 °C, with rates being one-half to one-third lower than at 37 °C (data not shown but example rates in Table 1). From these results, we see that the effects of gp41 peptide were

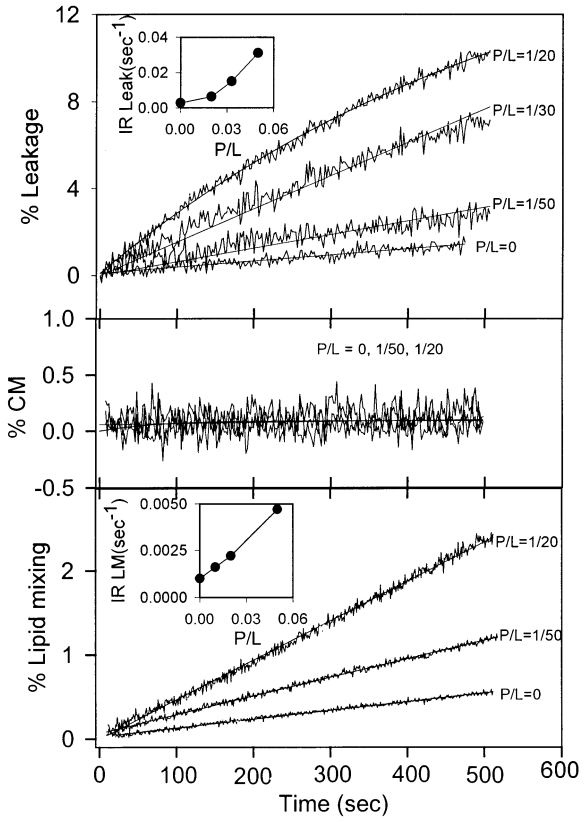

FIGURE 3: Time courses of (A) lipid mixing, (B) contents mixing, and (C) leakage for PC/PE/SM/CH (35:30:15:20) SUV induced by the gp41 fusion peptide at 37 °C. Measurements ware carried out using 200 μM SUVs in 10 mM TES, 100 mM NaCl, 1 mM $CaCl_2$, and 1 mM EDTA, pH 7.4. Representative results are shown for different P/L ratios. Insets show the initial rates of leakage and lipid mixing versus P/L ratio. Peptide surface occupancies under the conditions of these experiments varied from 0% to 36%.

qualitatively similar for optimally fusogenic and stable DOPC/DOPE/SM/CH vesicles as for unstable DOPC/DOPE/CH vesicles, although the magnitude of effects on unstable vesicles was much greater than for stable vesicles.

We also monitored the influence of gp41 peptide on particle size by QELS to detect aggregation of vesicles (Figure 4). In agreement with the lipid mixing data in Figure 3A, the ability of gp41 fusion peptide to aggregate vesicles was also minimal at low peptide concentration (P/L < 1:100), but it increased at high concentrations (P/L > 1:50), as can be seen from the variation of mean particle diameter as a function of P/L ratios in Figure 4.

To judge the effect of membrane curvature, similar experiments were performed with DOPC/DOPE/SM/CH LUVs (data not shown), with comparable results except that LUVs were, as expected, intrinsically a bit more leaky than SUVs and the effects of peptide on leakage and lipid mixing were somewhat less dramatic. As for SUVs, absolutely no contents mixing was observed up to P/L = 1:20.

In summary, the gp41 fusion peptide did not induce contents mixing between SUVs or LUVs of either lipid composition at either 23 or 37 °C. It did, however, induce lipid mixing, aggregation, and leakage with rates that varied with lipid composition, temperature, and membrane curvature.

Effects of Fusion Peptide on PEG-Mediated SUV and LUV Fusion. To test our hypothesis that gp41 peptide might

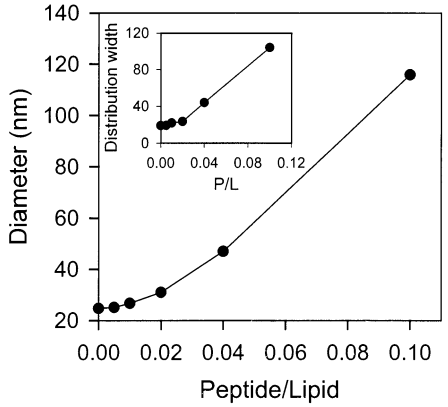

FIGURE 4: Effect of gp41 peptide on aggregation of PC/PE/SM/CH (35:30:15:20) SUVs. Peptide was added at increasing concentrations to vesicle suspensions (200 μM) and incubated for 10 min, after which QELS data were collected at 23 °C. The graph shows the mean particle diameter as a function of P/L ratio. The buffer was as described in Figure 1. The inset shows the width of Gaussian distribution of vesicle diameters as a function of the peptide/lipid ratio.

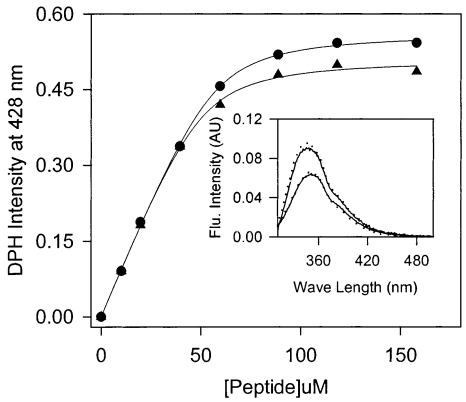

FIGURE 5: Effect of PEG on binding and emission spectra of gp41 fusion peptide. Peptide binding to DOPC SUVs was detected by energy transfer from Trp to DPH as a function of peptide concentration at 23 °C. Measurements were carried out using 200 μM SUV in 10 mM TES, 100 mM NaCl, 1 mM Ca^{2+}, and 1 mM EDTA at pH 7.4 in the presence (circles) and absence (triangles) of 10 wt % PEG. The smooth curve drawn through the data represents the best fit to a simple membrane-binding model (*32*) with a fixed stoichiometry of 4, yielding estimates of K_d of 3.2 ± 0.7 and 3.4 ± 0.7 μM in the presence and absence of PEG, respectively. The inset shows the emission spectra (excitation at 280 nm) of peptide in buffer and in a PC/PE/SM/CH SUV suspension in the presence (dotted lines) and absence (solid lines) of 5% PEG. Measurements were carried out using 200 μM SUV and 1 μM peptide in the same buffer as above.

influence fusion of PEG-aggregated vesicles, we first examined the effect of PEG on three aspects of peptide physical properties: binding to membranes, Trp emission spectrum, and depth of penetration into membranes. Figure 5 shows the increase in fluorescence intensity of membrane-bound DPH as a result of energy transfer from the bound peptide's Trp residue with increasing peptide concentration in the presence (circles) and absence (triangles) of 10 wt % PEG. In this experiment, we used DOPC SUVs because these do not fuse up to 15% PEG (*71*), meaning that our results reflect only binding and are uncomplicated by fusion. Binding parameters were obtained from the data using a single-site binding model (*32*). The apparent K_d's providing a best fit to the data were 3.2 ± 0.7 and 3.4 ± 0.7 in the presence and absence of PEG, respectively. Thus, PEG had no effect on peptide binding to membranes. Next, the inset to Figure 5 shows the emission spectrum of F8W gp41 peptide when it binds to PC/PE/SM/CH vesicles and in buffer in the presence (dotted curves) and absence (solid curves) of 5% (w/w) PEG. A blue shift and intensity enhancement were observed for peptide in the hydrophobic environment of the membrane, as expected if the single Trp of the F8W fusion peptide inserts at least partially into the SUV membrane. The fact that the λ_{max} shift and intensity change were the same in the presence and absence of PEG shows that the Trp environment in solution and on a membrane is unaffected by the presence of 5 wt % PEG. The environment of a single Trp at position 14 of a similar fusion peptide from influenza virus is dramatically altered (20 nm blue shift) by a pH-induced structural change in solution (coil → helix) (*53*). This argues that any significant change in F8W gp41 fusion peptide structure due to the presence of PEG should be reflected in a change in Trp fluorescence. Finally, we measured the depth of fusion peptide (tryptophan residue) penetration inside PC/PE/SM/CH SUVs using brominated lipids (6,7-Br_2-PC and 11,12-Br_2-PC) in the presence and absence of PEG (5% w/w) following the parallax method of fluorescence quenching (*10*). The distance of the single Trp residue from the center of the bilayer was 8.77 and 8.67 ± 0.06 Å in the absence and presence of PEG, respectively. While none of these measurements is designed to establish the structure of the peptide in solution or on a membrane, they do confirm that the presence of the low concentrations of PEG used in our experiments does not alter in any measurable way the nature of the peptide−membrane complex or the physical state of the peptide in solution.

Figure 6 shows representative data for the effects of fusion peptide on time courses of (A) contents mixing, (B) leakage, and (C) lipid mixing in DOPC/DOPE/SM/CH SUVs in the presence of 5% PEG at 23 °C. We focused on *stable DOPC/DOPE/SM/CH SUVs at 23 °C*, because leakage from DOPC/DOPE/CH vesicles was so great as to make it impossible to monitor fusion, because high temperature promotes contents leakage, and because we observed that curvature was necessary to observe a fusion-enhancing effect for HA fusion peptide (*23*). Contents mixing time courses were well described by a single exponential in the absence of peptide and at low peptide concentrations (P/L = 1:1600 and 1:800) and by a double exponential at higher peptide concentrations (P/L > 1:800). Lipid mixing time courses were always best described by two exponents, while a single exponential provided a good description of leakage time courses (except at P/L = 1:25).

Exponential analysis of time courses of events associated with the fusion process provides much more insight into the process than does end-point analysis of the extent of fusion, which we have shown reflects mainly the size of PEG-mediated vesicles aggregates (*21*, *77*). The kinetic constants (k_1 and k_2) and preexponential factors (*a* and *b*) from exponential descriptions of time courses such as shown in Figure 6 are summarized in Table 2 and were used (see legend to Figure 7) to obtain the initial rates of contents mixing (A, closed circles), leakage (A, closed triangles), and lipid mixing (B, closed circles) shown in Figure 7 as a function of P/L ratio. These results show that the initial rate of contents mixing and lipid mixing associated with PEG-

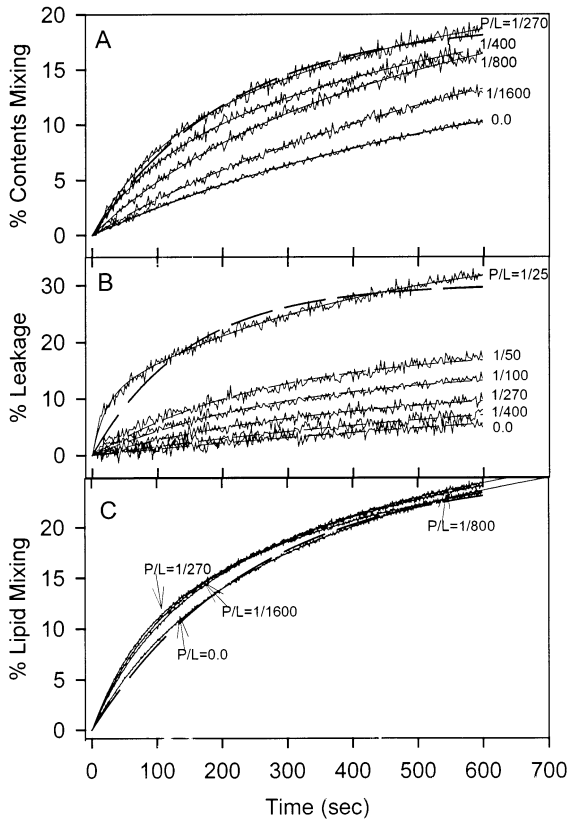

FIGURE 6: Effect of fusion peptide on the kinetics of (A) contents mixing, (B) leakage, and (C) lipid mixing in PC/PE/SM/CH (35:30:15:20) SUVs in the presence of 5 wt % PEG at 23 °C. Representative time courses are shown for different L/P ratios. Measurements ware carried in 10 mM TES, 100 mM NaCl, 1 mM $CaCl_2$, and 1 mM EDTA, pH 7.4. The smooth curves drawn through the data represent single (dashed lines) and double (solid lines) exponential fits.

mediated fusion of DOPC/DOPE/SM/CH SUVs increased by 4- and 1.7-fold, respectively, when vesicles were treated with fusion peptide up to a P/L of 1:267, while the rate of contents leakage was unchanged. The increase in the initial rate of contents mixing was primarily due to the appearance of a pore that formed on the time scale of the fast component of lipid mixing, except at P/L ratios of 1:1600 and 1:800, where such a fast pore could not be detected (see Table 2). From the binding constants measured in Figure 1, we estimated that the surface occupancy under these conditions is 3%. The initial rate of contents mixing between SUVs decreased, the rate of lipid mixing leveled off, and the rate of contents leakage increased dramatically above this very low surface occupancy (Figure 7). We conclude that the gp41 fusion peptide alone cannot induce vesicle fusion, but it can enhance PEG-mediated fusion of aggregated, fusogenic SUVs when it is present at low surface occupancies.

This behavior of gp41 fusion peptide is quite reminiscent of the behavior we have seen for the HA fusion peptide, whose effect on PEG-aggregated vesicles depended on membrane curvature stress (*23*). To determine whether the gp41 fusion peptide also required curvature stress to promote fusion, we examined the effect of gp41 peptide on PEG-induced leakage and contents mixing of DOPC/DOPE/SM/CH LUVs at a somewhat higher PEG concentration (12 wt %), since this is the threshold PEG concentration needed to induce fusion of these vesicles (*24*). These time courses (data not shown) were all well described by single exponentials, with initial rates also recorded in Figure 7A (open symbols). For LUVs, the rate of leakage (open triangles) increased substantially with added peptide without any increase in the very low rate of contents mixing (open circles) being observed at any P/L ratio. These results show clearly that the fusion-enhancing ability of gp41 fusion peptide, like that of HA fusion peptide, is dependent on membrane curvature stress.

Combined Effect of gp41 Fusion Peptide and N-Hexadecane. Hydrocarbons are assumed to relieve hydrophobic mismatch within high-energy intermediate states of the fusion process and, therefore, to enhance fusion of cells and vesicles (*2*, *12*, *72*). The effects of hexadecane on the initial rates of contents mixing, lipid mixing, and leakage are shown in Figure 7B,C as a function of P/L ratio, and the exponential constants from which these rates were obtained are recorded in Table 2. In the absence of fusion peptide, addition of hexadecane caused nearly a 10-fold increase in the initial rate of contents mixing (Table 2) due primarily to the appearance of a rapid exponential contents mixing component in addition to the slow component seen in the absence of hexadecane (Table 2). Only small increases in the initial rate of contents leakage (filled triangles in Figure 7C) or lipid mixing (Figure 7B, inverted triangles) were detected upon addition of hexadecane. Upon addition of gp41 fusion peptide in the presence of hexadecane, the rate as well as the extent of contents mixing actually decreased, and the rate of contents leakage was essentially unchanged. Significantly, however, the initial rate of lipid mixing was increased by about the same extent seen in the absence of hexadecane (~30%). The extent of lipid mixing was essentially unaffected by the presence of fusion peptide, but it was increased by the presence of hexadecane, meaning that fusion peptide and hexadecane affected PEG-mediated aggregation differently.

DISCUSSION

This paper has addressed several questions stated in the introduction. Here we pose answers to these questions.

gp41 Peptide Does Not Induce Fusion. The answer to the first of our questions is clear from our results (Figures 2 and 3) and is in agreement with results from other laboratories (*1*, *31*, *50*, *58*−*63*, *67*, *70*), except that we must disagree with the conclusion expressed by others that these observations correspond to "leaky fusion" (*50*, *52*, *60*). We corrected for contents leakage and still found no evidence of contents mixing, ruling out the possibility that gp41 fusion peptide promotes fusion of unaggregated vesicles. This conclusion was independent of vesicle concentration and temperature, although high temperature and inherently unstable vesicles made the membrane-disruptive properties of the gp41 peptide more evident.

gp41 Peptide Enhances Fusion of Aggregated Vesicles. As mentioned in the introduction, the observation by Nieva et al. of fusion of POPG LUVs in the presence of Ca^{2+} is the only case for which gp41 fusion peptide has been shown clearly to induce fusion (*58*). These authors suggested that the requirement for Ca^{2+} was both to aggregate (but not fuse) the POPG vesicles and to put the peptide in a fusogenic conformation. To distinguish between these two possible

Table 2: Kinetic Parameters for Fusion of PC/PE/SM/CH (35:30:15:20) SUV at 5% PEG in the Absence and Presence of Hexadecane at Different Lipid/Peptide (L/P) Ratios[a]

L/P	a	k_1	b	k_2	$a + b$	IR
			Contents Mixing			
∞			16.46 ± 0.20	$(164 \pm 2.8) \times 10^{-5}$	16.5	0.027
1600			20.91 ± 0.33	$(166 \pm 3.7) \times 10^{-5}$	20.9	0.035
800			20.62 ± 0.17	$(258 \pm 3.8) \times 10^{-5}$	20.6	0.053
400	5.85 ± 1.5	$(11.2 \pm 1.9) \times 10^{-3}$	18.55 ± 1.23	$(152 \pm 0.6) \times 10^{-5}$	24.4	0.093
267	5.75 ± 1.4	$(12.7 \pm 2.2) \times 10^{-3}$	17.26 ± 0.42	$(231 \pm 0.4) \times 10^{-5}$	23.0	0.113
160	7.04 ± 1.0	$(9.21 \pm 0.3) \times 10^{-3}$	14.12 ± 0.30	$(118 \pm 0.5) \times 10^{-5}$	21.6	0.081
			Contents Mixing in the Presence of 5 mol % Hexadecane			
∞	6.20 ± 0.04	$(33.6 \pm 3.9) \times 10^{-3}$	9.36 ± 0.12	$(215 \pm 7.1) \times 10^{-5}$	15.6	0.23
1000	5.37 ± 0.05	$(35.3 \pm 7.1) \times 10^{-3}$	8.96 ± 0.14	$(197 \pm 7.6) \times 10^{-5}$	14.3	0.21
200	4.41 ± 0.48	$(29.2 \pm 6.4) \times 10^{-3}$	9.66 ± 0.09	$(216 \pm 6.2) \times 10^{-5}$	14.1	0.15
100	3.81 ± 0.05	$(22.7 \pm 7.4) \times 10^{-3}$	9.23 ± 0.10	$(219 \pm 7.2) \times 10^{-5}$	13.0	0.11
			Lipid Mixing			
∞	5.56 ± 0.40	$(11.6 \pm 2.3) \times 10^{-3}$	24.24 ± 0.15	$(22.8 \pm 1.6) \times 10^{-4}$	29.8	0.120
1600	7.72 ± 0.23	$(12.9 \pm 0.3) \times 10^{-3}$	22.15 ± 0.09	$(23.4 \pm 0.5) \times 10^{-4}$	30.0	0.152
800	8.43 ± 0.27	$(13.6 \pm 0.3) \times 10^{-3}$	22.15 ± 0.08	$(23.1 \pm 0.8) \times 10^{-4}$	30.6	0.163
400	8.57 ± 0.22	$(15.2 \pm 0.3) \times 10^{-3}$	19.11 ± 0.08	$(25.0 \pm 0.7) \times 10^{-4}$	27.7	0.178
267	8.09 ± 0.20	$(19.4 \pm 0.4) \times 10^{-3}$	18.65 ± 0.07	$(29.5 \pm 0.8) \times 10^{-4}$	26.7	0.212
160	8.68 ± 0.21	$(20.5 \pm 0.4) \times 10^{-3}$	16.82 ± 0.08	$(26.5 \pm 0.8) \times 10^{-4}$	25.5	0.223
100	7.55 ± 0.12	$(23.8 \pm 0.4) \times 10^{-3}$	14.40 ± 0.05	$(30.9 \pm 0.8) \times 10^{-4}$	21.9	0.223
			Lipid Mixing in the Presence of 5 mol % Hexadecane			
∞	4.53 ± 1.09	$(18.5 \pm 1.6) \times 10^{-3}$	33.6 ± 0.33	$(23.2 \pm 1.6) \times 10^{-4}$	38.13	0.16
1000	3.98 ± 0.33	$(23.9 \pm 1.0) \times 10^{-3}$	29.6 ± 0.11	$(25.9 \pm 0.7) \times 10^{-4}$	33.58	0.17
200	7.88 ± 0.66	$(18.7 \pm 0.6) \times 10^{-3}$	27.6 ± 0.19	$(24.1 \pm 1.3) \times 10^{-4}$	35.48	0.21
100	7.71 ± 0.59	$(21.4 \pm 0.6) \times 10^{-3}$	27.0 ± 0.18	$(27.1 \pm 1.4) \times 10^{-4}$	34.71	0.24

[a] Data were fit to a single or double exponential using Sigma Plot 2000 (see legend of Figure 7), with a and b being the preexponential factors and k_1 and k_2 the exponential constants. IR indicates initial rate. Parameter errors were obtained from the fitting.

roles of Ca^{2+}, we have examined the effect of gp41 peptide on fusion of vesicles aggregated by PEG. PEG reduces the activity of water and thereby causes membrane dehydration leading to vesicle aggregation (*40*). PEG at the low concentrations used here has two effects on vesicles that help promote fusion: (1) aggregation of vesicles without interacting directly with them and (2) creating a compressive osmotic stress that makes vesicles more fusogenic (*46*). However, a compressive osmotic stress is not the major effect of PEG, since, even in the absence of an osmotic gradient, PEG-induced aggregation of fusogenic vesicles causes fusion (*46*). Since interbilayer contact resulting from aggregation is a clear prerequisite for fusion, the ability of PEG to aggregate and fuse PC/PE/SM/CH vesicles allows us to examine the effects of low (nonaggregating) concentrations of gp41 peptide on fusion while avoiding the complication of high, membrane-disrupting gp41 peptide concentrations.

Our results, summarized in Figure 7, demonstrate that gp41 peptide does promote fusion of aggregated vesicles at low peptide surface occupancy. These results, along with our conclusion that gp41 peptide does not promote fusion of unaggregated vesicles, argue that vesicle aggregation may have been one of the most important contributions of Ca^{2+} to the peptide-induced fusion reported by Nieva et al. As for the possibility that Ca^{2+} produced a fusogenic peptide conformation, we have been unable to detect any PEG-induced conformational change of gp41 fusion peptide in solution or associated with a membrane (see Results and Figure 5).

Curvature Stress Is Required for the Fusion-Promoting Effect of gp41 Peptide. Our results, summarized in Figure 7, demonstrate that membrane curvature stress is required to observe the fusion-enhancing capability of gp41 fusion peptide, just as we have observed for the HA fusion peptide (*23*). Yet, the majority of the reports on the membrane perturbing effects of gp41 and HA fusion peptide have used LUVs, not SUVs. Curiously, the clear report of Nieva et al. of fusion enhancement by gp41 fusion peptide was obtained with Ca^{2+}-aggregated POPG LUVs (*58*). Is this observation inconsistent with our conclusion that curvature stress is needed to observe the fusogenic potential of gp41 peptide? We think not. Aside from aggregating POPG vesicles, Ca^{2+} probably induced in these vesicles curvature stress similar to that experienced in the outer leaflet of SUVs. This is because POPG has a large effective headgroup cross section due to electrostatic repulsion (*20*), and Ca^{2+}, which induces hexagonal phases in pure PG dispersions (*25*), could well induce curvature stress in the outer leaflet of POPG LUV. Removal of outer leaflet lipid, ion-induced condensation of charged lipid headgroups, and curvature stress all promote PEG-mediated fusion (*37*, *71*). This requirement for curvature stress is completely reasonable given what we know about viral membrane fusion. An elegant freeze−fracture electron microscopy study of influenza virus fusion with liposomes shows fusion pore formation at the apex of highly curved dimpled membrane protrusions, suggesting that curvature stress is important to the induction of fusion by viral fusion machines (*30*). It is not known how the dimples arise, although many in the field believe that it is through mechanical work done on the membranes by the fusion protein machinery (*33*).

How Fusion Peptide Promotes Fusion. Although not universally accepted (*3*, *4*), the "stalk" model of the fusion process (*34*) is supported by a number of observations and is widely used as a working hypothesis. Figure 8 shows the presumed sequence of lipid rearrangements leading to membrane fusion within this model (*13*, *14*, *34*, *38*, *66*). An initial intermediate (S_1) is formed in a step that alters

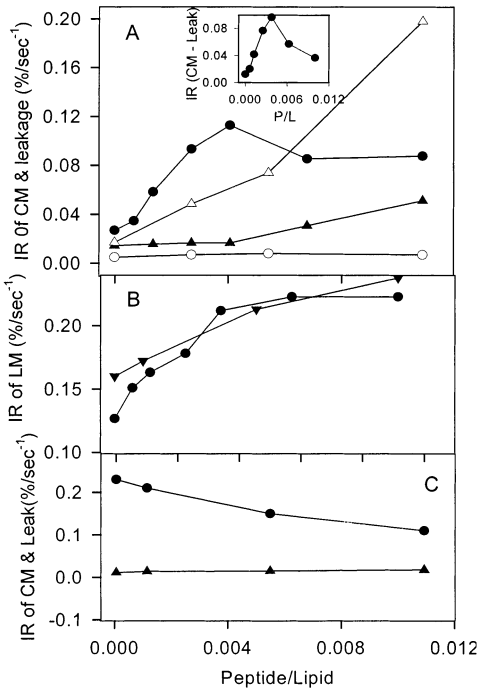

FIGURE 7: Influence of peptide on the initial rate of PEG-mediated (A) contents mixing (circles) and leakage (triangles) and (B) lipid mixing in PC/PE/SM/CH (35:30:15:20) vesicles. The experimental condition was the same as in Figure 6 except that the PEG concentration was 12 wt % for LUVs (open symbols) and 5 wt % for SUVs (closed symbols). The inset to frame A shows the difference in the initial rate of contents mixing and leakage of SUVs as a function of peptide/lipid ratio. Time courses such as shown in Figure 6 were fit to a single exponential [$f = a(1 - \exp(-kx))$, with initial rate ak] for leakage and to a double exponential [$f = a(1 - \exp(-k_1x)) + b(1 - \exp(-k_2x))$, with initial rate $ak_1 + bk_2$] for contents mixing and lipid mixing. Errors in the rates of lipid mixing and contents mixing from repeats with a single vesicle preparation were 5−8%. The effects of hexadecane on lipid mixing (inverted triangles in frame B) and contents mixing and leakage of SUVs (filled circles and triangles, respectively, in frame C) are also given. Hexadecane at 5 mol % of the lipid concentration was added to the lipid mixture before lyophilization.

membrane topology away from the normal bilayer morphology. The probability of this event depends on the distance of interbilayer approach and on events or processes that disrupt packing of the approaching membrane leaflets (*7*, *37*). Fusion peptides are widely viewed as favoring fusion by disrupting bilayer packing and perhaps favoring formation of such a nonbilayer intermediate (*15*, *53*, *61*). This first step of the process is marked by mixing of lipids between contacting or outer leaflets of fusing membranes (*21*, *38*). In 45 nm vesicles, we have resolved a distinct second intermediate (presumably structures such as S_2 or S_3) (*36*). A distinct intermediate process between S_1 and pore formation (S_4) was not detectable in 25 nm vesicles, although the need for two exponentials to describe the time course of lipid mixing demonstrates the existence of at least one intermediate (*21*). A transient or minimal pore is also associated with the initial intermediate (*36*) and is detectable as a fast component of contents mixing in extensively fusing systems (*21*). Evolution of S_1 to a pre-pore structure (S_2 or S_3) involves rearrangements in nonbilayer structures without a change in membrane topology. The appearance and subsequent disappearance of nonbilayer structures have been detected using pyrene-labeled cholesterol ester (*48*). The free energy of these

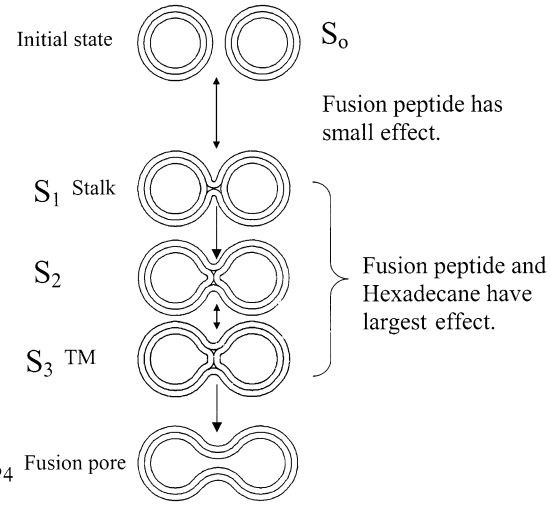

FIGURE 8: Effect of gp41 fusion peptide on the stages of the fusion process. A description of the stages of fusion is given in the Discussion. Our results suggest that gp41 fusion peptide enhances the rate of the first step (1.7-fold at 23 °C) but mainly that of the second or third steps (>4-fold).

continuously evolving lipidic intermediates is dominated by monolayer bending free energy and the very unfavorable free energy of the regions of "hydrophobic mismatch" shown as shaded areas in Figure 8 (*44*, *66*). Once an initial intermediate is formed, the lipid system must overcome the unfavorable hydrophobic mismatch free energy in order to evolve to a point from which it can form a stable fusion pore ($S_3 \rightarrow S_4$), the final and topologically discontinuous step (*38*). There is a good correspondence between this kinetic model, developed for PEG-mediated fusion of liposomes, and the kinetics of fusion reported in exocytotic or viral fusion model systems (*38*).

The membrane-disruptive ability of the gp41 fusion peptide is widely described in the literature as the basis of the role of fusion peptide in viral fusion. It has been shown that mutations in gp41 fusion peptide that interfere with viral fusion also reduce the membrane disruption ability of a matching synthetic 33-residue peptide (*62*), lending credence to this possibility. In agreement with this view, our results show that the initial rate of lipid mixing was increased by gp41 fusion peptide by about 30%. This probably reflects the influence of gp41 peptide on the initial step of the fusion process (Figure 8).

In addition, enhancing the rate of the first step of the fusion process, gp41 peptide increased by more than 4-fold the rate of contents mixing (Figure 7 and Table 2). This means that the later steps of the fusion process ($S_1 \rightarrow S_4$) were more affected by fusion peptide than was the first step (Figure 8). By examining mutations in the fusion peptide region of whole HA, Schoch et al. (*64*) suggested that the HA fusion peptide plays a vital role in later stages in the fusion process (pore widening). Although no comparable study of the fusion peptide region of gp41 has been made, this report establishes that the fusion peptide region of fusion proteins plays a significant role in pore formation in vivo. Our results clearly show that the major effect of synthetic fusion peptide is on pore formation.

How might fusion peptide enhance pore formation? Our results show that fusion peptide increases the rate of pore formation mainly by promoting formation of a minor but

rapid component of contents mixing, on the same time scale of the rapid component of lipid mixing (Table 2). Our interpretation is that the gp41 fusion peptide stabilizes and promotes formation of an initial unstable pore associated with formation of the initial intermediate.

What molecular property of the gp41 fusion peptide might account for this ability to promote formation of a rapid pore directly from the initial intermediate? Hexadecane, like the fusion peptide, also promoted rapid pore formation. In addition, hexadecane masked the pore-promoting effect of gp41 fusion peptide (compare initial rates of contents mixing for peptide-free vesicles and vesicles with a P/L of 1:1000 in the presence of hexadecane in Table 2). The role of hexadecane in promoting fusion is believed to be in stabilizing nonlamellar structures (*12*) and thereby promoting pore formation (*2*, *72*). A reasonable interpretation of these observations is that both hexadecane and gp41 fusion peptide might lower the activation energy for pore formation by compensating for packing defects that necessarily accompany nonlamellar structures. The gp41 fusion peptide possesses a conserved hydrophobic FLGFL motif (residues 8−12) that is critical to gp41-mediated fusion (*62*). We suggest that this conserved hydrophobic sequence might insert into nonlamellar structures and stabilize them to lower the activation energy for conversion of the initial intermediate to a pore.

Finally, we note that, while the ability of the gp41 fusion peptide to destabilize, aggregate, and mix outer leaflets of neutral lipid vesicles is of smaller magnitude than for the HA fusion peptide (*23*), the abilities of these two fusion peptides to enhance fusion of PEG-aggregated vesicles are qualitatively similar. This suggests that N-terminal fusion peptides of different viruses may function similarly in the fusion process.

ACKNOWLEDGMENT

We thank Dr. Vladimir Malinin for helpful discussion.

REFERENCES

1. Agirre, A., Flach, C., Goni, F. M., Mendelsohn, R., Valpuesta, J. M., Wu, F., and Nieva, J. L. (2000) *Biochim. Biophys. Acta 1467*, 153−164.
2. Basanez, G., Goni, F. M., and Alonso, A. (1998) *Biochemistry 37*, 3901−3908.
3. Bentz, J. (2000) *Biophys. J. 78*, 886−900.
4. Bonnafous, P., and Stegmann, T. (2000) *J. Biol. Chem. 275*, 6160−6166.
5. Bosch, M. L., Earl, P. L., Fargnoli, K., Picciafuoco, S., Giombini, F., Wong-Staal, F., and Franchini, G. (1989) *Science 244*, 694−697.
6. Brunner, J. (1989) *FEBS Lett. 257*, 369−372.
7. Burgess, S. W., McIntosh, T. J., and Lentz, B. R. (1992) *Biochemistry 31*, 2653−2661.
8. Chan, D. C., Fass, D., Berger, J. M., and Kim, P. S. (1997) *Cell 89*, 263−273.
9. Chanturiya, A., Leikina, E., Zimmerberg, J., and Chernomordik, L. V. (1999) *Biophys. J. 77*, 2035−2045.
10. Chattopadhyay, A., and London, E. (1987) *Biochemistry 26*, 39−45.
11. Chen, P. S., Jr., Toribara, T. Y., and Warner, H. (1956) *Anal. Chem. 28*, 1756−1758.
12. Chen, Z., and Rand, R. P. (1998) *Biophys. J. 74*, 944−952.
13. Chernomordik, L., Kozlov, M. M., and Zimmerberg, J. (1995) *J. Membr. Biol. 146*, 1−14.
14. Chernomordik, L. V., Melikyan, G. B., and Chizmadzhev, Y. A. (1987) *Biochim. Biophys. Acta 906*, 309−352.
15. Colotto, A., and Epand, R. M. (1997) *Biochemistry 36*, 7644−7651.
16. Curtain, C., Separovic, F., Nielsen, K., Craik, D., Zhong, Y., and Kirkpatrick, A. (1999) *Eur. Biophys. J. 28*, 427−436.
17. Dimitrov, D. S. (1997) *Cell 91*, 721−730.
18. Dimitrov, D. S., Golding, H., and Blumenthal, R. (1991) *AIDS Res. Hum. Retroviruses 7*, 799−805.
19. Epand, R. F., Macosko, J. C., Russell, C. J., Shin, Y. K., and Epand, R. M. (1999) *J. Mol. Biol. 286*, 489−503.
20. Epand, R. M., and Hui, S. W. (1986) *FEBS Lett. 209*, 257−260.
21. Evans, K. O., and Lentz, B. R. (2002) *Biochemistry 41*, 1241−1249.
22. Freed, E. O., Myers, D. J., and Risser, R. (1990) *Proc. Natl. Acad. Sci. U.S.A. 87*, 4650−4654.
23. Haque, M. E., McCoy, A. J., Glenn, J., Lee, J., and Lentz, B. R. (2002) *Biochemistry* (in press).
24. Haque, M. E., McIntosh, T. J., and Lentz, B. R. (2001) *Biochemistry 40*, 4340−4348.
25. Harlos, K., and Eibl, H. (1980) *Biochim. Biophys. Acta 601*, 113−122.
26. Hope, M. J., Bally, M. B., Webb, G., and Cullis, P. R. (1985) *Biochim. Biophys. Acta 812*, 55−65.
27. Huang, C., and Mason, J. T. (1978) *Proc. Natl. Acad. Sci. U.S.A. 75*, 308−310.
28. Hunter, E., and Swanstrom, R. (1990) *Curr. Top. Microbiol. Immunol. 157*, 187−253.
29. Jones, J. D., and Thompson, T. E. (1990) *Biochemistry 29*, 1593−1600.
30. Kanaseki, T., Kawasaki, K., Murata, M., Ikeuchi, Y., and Ohnishi, S. (1997) *J. Cell Biol. 137*, 1041−1056.
31. Kliger, Y., Aharoni, A., Rapaport, D., Jones, P., Blumenthal, R., and Shai, Y. (1997) *J. Biol. Chem. 272*, 13496−13505.
32. Koppaka, V., and Lentz, B. R. (1996) *Biophys. J. 70*, 2930−2937.
33. Kozlov, M. M., and Chernomordik, L. V. (1998) *Biophys. J. 75*, 1384−1396.
34. Kozlov, M. M., Leikin, S. L., Chernomordik, L. V., Markin, V. S., and Chizmadzhev, Y. A. (1989) *Eur. Biophys. J. 17*, 121−129.
35. Kwong, P. D., Wyatt, R., Robinson, J., Sweet, R. W., Sodroski, J., and Hendrickson, W. A. (1998) *Nature 393*, 648−659.
36. Lee, J., and Lentz, B. R. (1997) *Biochemistry 36*, 6251−6259.
37. Lee, J., and Lentz, B. R. (1997) *Biochemistry 36*, 421−431.
38. Lee, J., and Lentz, B. R. (1998) *Proc. Natl. Acad. Sci. U.S.A. 95*, 9274−9279.
39. Leikina, E., Markovic, I., Chernomordik, L. V., and Kozlov, M. M. (2000) *Biophys. J. 79*, 1415−1427.
40. Lentz, B. R. (1994) *Chem. Phys. Lipids 73*, 91−106.
41. Lentz, B. R., Carpenter, T. J., and Alford, D. R. (1987) *Biochemistry 26*, 5389−5397.
42. Lentz, B. R., Malinin, V., Haque, M. E., and Evans, K. (2000) *Curr. Opin. Struct. Biol. 10*, 607−615.
43. Lentz, B. R., McIntyre, G. F., Parks, D. J., Yates, J. C., and Massenburg, D. (1992) *Biochemistry 31*, 2643−2653.
44. Lentz, B. R., Siegel, D. P., and Malinin, V. (2002) *Biophys. J. 82*, 555−557.
45. Lu, M., Ji, H., and Shen, S. (1999) *J. Virol. 73*, 4433−4438.
46. Malinin, V. S., Frederik, P., and Lentz, B. R. (2002) *Biophys. J.* (in press).
47. Malinin, V. S., Haque, M. E., and Lentz, B. R. (2002) *Biochemistry* (in press).
48. Malinin, V. S., and Lentz, B. R. (2002) *Biochemistry 41*, 5913−5919.
49. Markosyan, R. M., Melikyan, G. B., and Cohen, F. S. (1999) *Biophys. J. 77*, 943−952.
50. Martin, I., Defrise-Quertain, F., Decroly, E., Vandenbranden, M., Brasseur, R., and Ruysschaert, J. M. (1993) *Biochim. Biophys. Acta 1145*, 124−133.
51. Martin, I., Defrise-Quertain, F., Mandieau, V., Nielsen, N. M., Saermark, T., Burny, A., Brasseur, R., Ruysschaert, J. M., and Vandenbranden, M. (1991) *Biochem. Biophys. Res. Commun. 175*, 872−879.
52. Martin, I., and Ruysschaert, J. M. (1997) *FEBS Lett. 405*, 351−355.
53. Matsumoto, T. (1999) *Biophys. Chem. 79*, 153−162.
54. Mayer, L. D., Hope, M. J., and Cullis, P. R. (1986) *Biochim. Biophys. Acta 858*, 161−168.
55. McIntosh, T. J., and Holloway, P. W. (1987) *Biochemistry 26*, 1783−1788.
56. Melikyan, G. B., and Chernomordik, L. V. (1997) *Trends Microbiol. 5*, 349−355.

57. Moore, J. P., Jameson, B. A., Weiss, R. A., and Sattentau, Q. J. (1993) *Viral Fusion Mechanisms*, pp 233−289, CRC Press, Boca Raton, FL.
58. Nieva, J. L., Nir, S., Muga, A., Goni, F. M., and Wilschut, J. (1994) *Biochemistry 33*, 3201−3209.
59. Peisajovich, S. G., Epand, R. F., Pritsker, M., Shai, Y., and Epand, R. M. (2000) *Biochemistry 39*, 1826−1833.
60. Pereira, F. B., Goni, F. M., Muga, A., and Nieva, J. L. (1997) *Biophys. J. 73*, 1977−1986.
61. Pereira, F. B., Valpuesta, J. M., Basanez, G., Goni, F. M., and Nieva, J. L. (1999) *Chem. Phys. Lipids 103*, 11−20.
62. Pritsker, M., Rucker, J., Hoffman, T. L., Doms, R. W., and Shai, Y. (1999) *Biochemistry 38*, 11359−11371.
63. Rafalski, M., Lear, J. D., and DeGrado, W. F. (1990) *Biochemistry 29*, 7917−7922.
64. Schoch, C., and Blumenthal, R. (1993) *J. Biol. Chem. 268*, 9267−9274.
65. Schwenk, E., and Werthessen, N. T. (1952) *Arch. Biochem. Biophys. 40*, 334−341.
66. Siegel, D. P. (1993) in *Viral Fusion Mechanisms* (Bentz, J., Ed.) pp 475−512, CRC Press, Boca Raton, FL.
67. Slepushkin, V. A., Andreev, S. M., Sidorova, M. V., Melikyan, G. B., Grigoriev, V. B., Chumakov, V. M., Grinfeldt, A. E., Manukyan, R. A., and Karamov, E. V. (1992) *AIDS Res. Hum. Retroviruses 8*, 9−18.
68. Stegmann, T., Bartoldus, I., and Zumbrunn, J. (1995) *Biochemistry 34*, 1825−1832.
69. Stryer, L. (1966) *J. Am. Chem. Soc. 88*, 5708−5712.
70. Suarez, T., Gallaher, W. R., Agirre, A., Goni, F. M., and Nieva, J. L. (2000) *J. Virol. 74*, 8038−8047.
71. Talbot, W. A., Zheng, L. X., and Lentz, B. R. (1997) *Biochemistry 36*, 5827−5836.
72. Walter, A., Yeagle, P. L., and Siegel, D. P. (1994) *Biophys. J. 66*, 366−376.
73. Weissenhorn, W., Dessen, A., Harrison, S. C., Skehel, J. J., and Wiley, D. C. (1997) *Nature 387*, 426−430.
74. White, J. M. (1990) *Annu. Rev. Physiol. 52*, 675−697.
75. Wilkinson, D. (1996) *Curr. Biol. 6*, 1051−1053.
76. Wilschut, J., Duzgunes, N., Fraley, R., and Papahadjopoulos, D. (1980) *Biochemistry 19*, 6011−6021.
77. Wu, J. R., and Lentz, B. R. (1991) *Biochemistry 30*, 6780−6787.

BI020269Q